

Thermodynamic origin of medium-entropy stabilization in multicomponent rock-salt oxides

Supriya Ghosal^a, Swapan Pati^a, and Ashutosh Kumar^{b,*}

^aTheoretical Sciences Unit, Jawaharlal Nehru Centre for Advanced Scientific Research, Bangalore, Karnataka 560064, India and

^bFunctional Materials Laboratory, Department of Materials Science and Metallurgical Engineering, Indian Institute of Technology Bhilai, Chhattisgarh 491002, India

(Dated: June 2, 2026)

High entropy oxides are commonly associated with high configurational entropy ($\Delta S_{conf} \geq 1.61R$) corresponding to five equimolar cations occupying a crystallographic sublattice. However, recent experimental observations indicate that medium-entropy compositions may also exhibit entropy-stabilized rock-salt phases, raising an important question regarding the minimum entropy required for phase stabilization. In this work, we employ a first-principles thermodynamic framework to investigate the stability of rock-salt oxides containing two to five principal cations components analogous to $(\text{Ni}_{0.8}\text{Cu}_{0.2})\text{O}$, $(\text{Ni}_{0.6}\text{Cu}_{0.2}\text{Zn}_{0.2})\text{O}$, $(\text{Ni}_{0.4}\text{Cu}_{0.2}\text{Zn}_{0.2}\text{Co}_{0.2})\text{O}$, $(\text{Ni}_{0.2}\text{Cu}_{0.2}\text{Zn}_{0.2}\text{Co}_{0.2}\text{Mg}_{0.2})\text{O}$. Density functional theory, MCSQS-based structural modeling, and finite-temperature Gibbs free-energy analysis are combined to quantify the roles of enthalpy mixing (ΔH_{mix}), configurational (ΔS_{conf}), vibrational (ΔS_{vib}), and electronic contributions towards (ΔS_{elec}) entropy change in governing phase stability. The results show that ΔS_{conf} alone is not a universal descriptor of phase stability. While the two-cation system is enthalpy-stabilized but three-, four- and five-cation systems become thermodynamically stable at high-temperature due to entropy-driven reduction of the Gibbs free energy. These findings demonstrate that single-phase rock-salt oxides are not restricted to the conventional high-entropy limit and that medium-entropy compositions can also be stabilized under suitable thermodynamic conditions.

High-entropy oxides (HEOx) have opened a new direction in the chemistry and physics of crystalline solids by extending the concept of multicomponent disorder from metallic systems to oxygen-mediated compounds. In these materials, several cations share a crystallographic sublattice in near-equimolar proportions, producing large chemical disorder within a still-crystalline framework. Unlike conventional substitutional oxides, where disorder is typically treated as a perturbation to a parent lattice, HEOx represent a regime in which disorder itself becomes a defining structural parameter. This has enabled access to unusual combinations of phase stability and functionality across a wide range of oxide systems.

The field of HEOx was catalyzed by the discovery of single-phase entropy stabilized oxide: $(\text{Mg,Co,Ni,Cu,Zn})\text{O}$, in which five cations were incorporated into one cationic sublattice and stabilized as a homogeneous solid solution at elevated temperature.[1] That discovery established a central idea in the field: a configurational entropy $\Delta S_{conf} \geq 1.6R$ can offset unfavorable enthalpic contributions and stabilize compositionally complex oxide phases that would otherwise decompose into simpler constituents. Since then, entropy-assisted stabilization has been explored in several oxide families, including rock-salt, fluorite[2], pyrochlore[3], and perovskite[4] structures, indicating that multicomponent cation disorder can serve as a general route toward structurally and functionally

diverse oxide materials.

Fracchia et al.[5] showed that rock-salt oxides with even medium ΔS_{conf} can display entropy-stabilized behavior, suggesting that the stabilization threshold may be substantially lower than the canonical five-component limit. This observation calls for a basic thermodynamic question that remains unresolved: how much ΔS_{conf} is actually required to stabilize a single-phase oxide? While the common operational definition of a high-entropy material is strictly mapped to an ideal equimolar five-component system ($\Delta S_{conf} \approx 1.61R$), [1, 6, 7] relaxed thresholds (e.g., $\Delta S_{conf} \geq 1.5R$) are widely accepted to accommodate non-equimolar deviations. Regardless of the exact threshold, a large configurational entropy alone does not necessarily prove entropy-stabilized phase formation. Also, It is important to distinguish between high-entropy oxides and entropy-stabilized oxides. A high-entropy oxide is usually classified based on compositional complexity and configurational entropy [8, 9], whereas an entropy-stabilized oxide is one in which the single-phase structure is stabilized specifically because the entropy contribution overcomes the positive enthalpy penalty for mixing[7, 10]. Therefore, a large ΔS_{conf} alone does not necessarily prove entropy-stabilized phase formation; rather, the stabilization must be evaluated from the temperature-dependent Gibbs free energy. This distinction is particularly important for medium-entropy oxides, where the configurational entropy is lower than the conventional high-entropy threshold but may still be sufficient to stabilize a single-phase oxide under suitable thermodynamic conditions.

More fundamentally, the stability of a multicomponent oxide may not be inferred from configurational entropy

*Email: ashutosh@iitbhilai.ac.in

alone. The relevant thermodynamic quantity is the Gibbs free energy of mixing, in which the enthalpy of mixing competes with temperature-dependent entropy contributions. In addition to configurational entropy, both vibrational and electronic entropy may influence the stabilization of compositionally complex oxides, particularly at elevated temperature. Therefore, whether a given rock-salt oxide forms a stable single phase depends on the collective balance among these contributions rather than on a nominal entropy classification alone. Resolving this issue is essential not only for clarifying the physical meaning of “entropy stabilization,” but also for establishing predictive principles for the design of compositionally complex oxides.

Here, we develop a first-principles framework to elucidate the thermodynamic phase stability of rock-salt oxides containing two to five principal cation components. Recent descriptor-based studies have also shown that the formation of single-phase multicomponent oxides cannot be predicted from configurational entropy alone.[11–13] These studies emphasize that parameters such as statistical variations in local mixing enthalpies (e.g., the Entropy-Forming Ability), cation-size mismatch (tolerance factors), preferred binary oxide ground states, and local bonding environments must be evaluated collectively. This motivates a more complete thermodynamic treatment in which ΔH_{mix} , ΔS_{conf} , ΔS_{vib} , and ΔS_{elec} are evaluated explicitly rather than assuming a fixed entropy threshold for phase stabilization. By combining density functional theory, lattice-dynamical analysis, and finite-temperature entropy contributions, we evaluate the respective roles of mixing enthalpy, configurational entropy, vibrational entropy, and electronic entropy in governing the Gibbs free energy of multicomponent oxide solid solutions. Through this comparative analysis, we show that the the medium configurational entropy can already be sufficient to stabilize a single-phase rock-salt oxide under appropriate thermodynamic conditions. These results refine our current understanding of entropy-stabilized oxides and provide a broader thermodynamic basis for designing single-phase compositionally complex oxides beyond the conventional high-entropy limit.

I. COMPUTATIONAL METHODS

Theoretical analyses were carried out using the first-principles density functional theory (DFT) framework as implemented in the Vienna *Ab-initio* Simulation Package (VASP)[14–16]. In order to describe ion-electron interactions accurately, the projector augmented-wave (PAW) method was employed in conjunction with the generalized gradient approximation (GGA) in the form of the Perdew-Burke-Ernzerhof (PBE) exchange-correlation functional[17, 18]. For structural optimizations, the unit cells were sampled using a $4 \times 4 \times 4$ Monkhorst-Pack

(MP) k -point grid in combination with a plane-wave cut-off energy of 600 eV[19]. The unit-cell structures were geometrically optimized until the residual force components converged below 10^{-3} eV/Å, with a total energy convergence tolerance of 10^{-7} eV for the self-consistent electronic loop.

Depending on the experimentally reported structure of NiO[20] with fractional occupancy, random structures were generated using the special quasi-random structures (SQS) method. SQS formalism uses the mcsqs code as implemented in the Alloy Theoretic Automated Toolkit (ATAT) routines[21–24]. The SQS algorithm is designed to minimize the correlation difference between a finite cell and the corresponding infinite random system. Thus, SQSs provide a suitable platform to approximate near-randomness in the properties of solid-solution alloys. For all four structures included in the theoretical study, a 60-atom supercell was used for the SQS structures by considering cutoff radii of 8 Å, 7 Å, and 6 Å for pair, three-body, and four-body correlations, respectively.

The SQS approach was used to approximate a random cation distribution on the rock-salt sublattice. However, it should be noted that the ideal configurational entropy expression assumes complete random mixing. In real multicomponent oxides, local chemical preferences and short-range ordering may reduce the effective configurational entropy. Therefore, the SQS-based results should be interpreted as a thermodynamic approximation to the disordered state.

To treat magnetic elements and their magnetic ground states accurately, spin-polarized calculations were incorporated with initialized magnetic moments. Since NiO, CoO, and CuO contain partially filled $3d$ orbitals, spin-polarized calculations were performed. The magnetic ground states of the binary reference oxides were considered while evaluating the mixing enthalpy. For NiO and CoO, antiferromagnetic ordering was used in accordance with their known ground states. The magnetic moments were initialized on transition-metal cations, and the final converged magnetic moments were checked after structural relaxation.

To assess phase stability, the change in Gibbs free energy of mixing, ΔG_{mix} , was calculated using the following relation[25]:

$$\Delta G_{\text{mix}} = \Delta H_{\text{mix}} - T\Delta S_{\text{mix}}. \quad (1)$$

Here, ΔH_{mix} and ΔS_{mix} represent the enthalpy change and entropy change of mixing, respectively. For a consistent thermodynamic comparison, all energetic and entropic quantities were normalized on a per-atom basis. The mixing enthalpy was evaluated with respect to the thermodynamically stable binary oxide reference phases using the same computational settings. The total entropy of mixing was considered as the sum of configurational, vibrational, and electronic entropy contributions:

$$\Delta S_{\text{mix}} = \Delta S_{\text{conf}} + \Delta S_{\text{vib}} + \Delta S_{\text{elec}}. \quad (2)$$

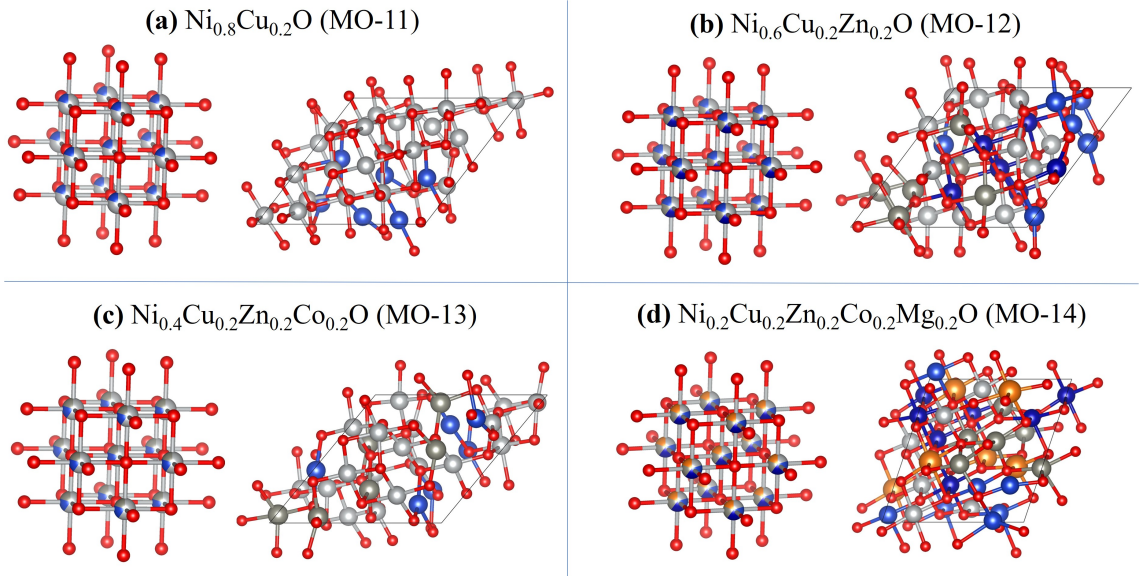


FIG. 1: Structural geometry of (a) $\text{Ni}_{0.8}\text{Cu}_{0.2}\text{O}$ (MO-11), (b) $\text{Ni}_{0.6}\text{Cu}_{0.2}\text{Zn}_{0.2}\text{O}$ (MO-12), (c) $\text{Ni}_{0.4}\text{Cu}_{0.2}\text{Zn}_{0.2}\text{Co}_{0.2}\text{O}$ (MO-13), (d) $\text{Ni}_{0.2}\text{Cu}_{0.2}\text{Zn}_{0.2}\text{Co}_{0.2}\text{Mg}_{0.2}\text{O}$ (MO-14) oxide systems. In each box, left panel and right panel showcase ordered crystalline and quasi-random disordered structures respectively.

Therefore, the temperature-dependent phase stability was assessed from the total Gibbs free energy of mixing rather than from configurational entropy alone.

The mixing enthalpy, ΔH_{mix} , was calculated using the following expression for a two-cation random solid solution decomposing into two one-cation oxides:

$$\Delta H_{\text{mix}} = E_{\text{DFT}}[(A_m A'_n)O_{m+n}] - mE_{\text{DFT}}[AO] - nE_{\text{DFT}}[A'O]. \quad (3)$$

Here, $E_{\text{DFT}}[(A_m A'_n)O_{m+n}]$, $E_{\text{DFT}}[AO]$, and $E_{\text{DFT}}[A'O]$ represent the ground-state total energies of the two-cation random solid solution $(A_m A'_n)O_{m+n}$ and the corresponding one-cation oxides AO and $A'O$, respectively. In a similar manner, the mixing enthalpy for a five-cation SQS structure was also calculated.

The mixing entropy includes contributions from configurational entropy, S_{conf} , vibrational entropy, S_{vib} , and electronic entropy, S_{elec} [25]. The change in mixing entropy represents the difference in entropy between the random solid-solution phase and the constituent binary oxides. The configurational entropy of the random solid solutions was calculated using:

$$S_{\text{conf}} = -R \sum_{i=1}^n x_i \ln x_i, \quad (4)$$

where x_i is the molar fraction of the i th cation on the cationic sublattice.

To calculate the vibrational entropy, phonon calculations were performed for the supercell. Based on the finite-displacement approach, a large number of displaced structures were generated using the Phonopy code[26].

The second-order interatomic force constants were obtained from static DFT calculations performed on multiple displaced configurations generated within a $2 \times 2 \times 2$ supercell. The dynamical matrix was constructed for different q -vectors in the Brillouin zone using the force-constant matrix. By solving the dynamical matrix, the eigenvalues of phonon frequencies and eigenvectors of phonon modes were obtained using the Phonopy package. The vibrational entropy was calculated by summing over all phonon modes using the following expression[27]:

$$S_{\text{vib}} = \frac{1}{2T} \sum_{qb} \hbar\omega(q, b) \coth \left[\frac{\hbar\omega(q, b)}{2k_{\text{B}}T} \right] - k_{\text{B}} \sum_{qb} \ln \left[2 \sinh \left(\frac{\hbar\omega(q, b)}{2k_{\text{B}}T} \right) \right]. \quad (5)$$

Here, \hbar , $\omega(q, b)$, k_{B} , and T represent the reduced Planck constant, phonon frequency for wave vector q and branch b , Boltzmann constant, and temperature, respectively.

The electronic contribution to entropy, S_{elec} , was calculated from the electronic density of states by considering the thermal excitation of electrons across the Fermi level[16]. The electronic entropy was evaluated using:

$$S_{\text{elec}} = -k_{\text{B}} \int N(\varepsilon) \left[f(\varepsilon) \ln f(\varepsilon) + \{1 - f(\varepsilon)\} \ln \{1 - f(\varepsilon)\} \right] d\varepsilon. \quad (6)$$

Here, k_{B} , $N(\varepsilon)$, and $f(\varepsilon)$ represent Boltzmann's constant, the electronic density of states, and the Fermi-Dirac distribution function, respectively. When finite-

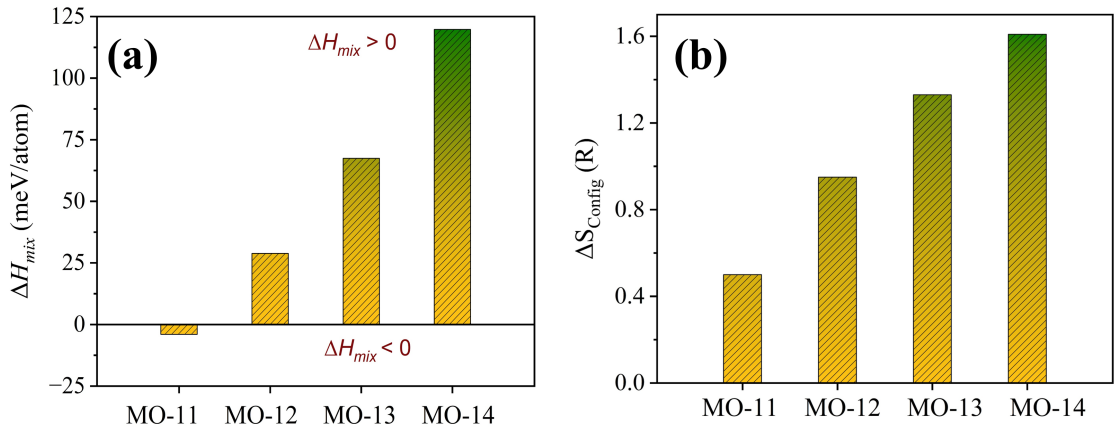


FIG. 2: (a) Enthalpy of mixing (ΔH_{mix}) in units of meV/atom and (b) configurational entropy change in units of the universal gas constant, $R \approx 8.63 \times 10^{-5} \text{ eV K}^{-1} \text{ atom}^{-1}$, for MO oxide solid-solution systems.

temperature electronic calculations were performed, the total electronic entropy was calculated as a time average over the equilibrated simulation trajectory:

$$S_{elec} = \langle S_{elec}(t) \rangle_t. \quad (7)$$

The change in entropy was then obtained as the difference between the entropy of the random solid-solution phase and the weighted entropy contributions of the corresponding constituent binary oxides.

II. RESULTS AND DISCUSSION

A. Mixing enthalpy of solid solutions

Theoretically, by means of first-principles DFT, ab-initio molecular dynamics (AIMD) and phonon calculations, thermodynamic phases of SQSs are analysed. For theoretical study, we have considered 4 oxide systems i.e. MO-11 ($\text{Ni}_{0.8}\text{Cu}_{0.2}\text{O}$), MO-12 ($\text{Ni}_{0.6}\text{Cu}_{0.2}\text{Zn}_{0.2}\text{O}$), MO-13 ($\text{Ni}_{0.4}\text{Cu}_{0.2}\text{Zn}_{0.2}\text{Co}_{0.2}\text{O}$), MO-14 ($\text{Ni}_{0.2}\text{Cu}_{0.2}\text{Zn}_{0.2}\text{Co}_{0.2}\text{Mg}_{0.2}\text{O}$), each containing 60 atoms in the supercell (Fig. 1).

From MO-11 to MO-14, the number of elements in the cationic site increases from 2 to 5. Absence of imaginary phonon frequencies in the phonon spectra confirms the dynamical stability of SQSs. Thus, dynamically stable SQSs truly reflect experimentally synthesized random solid solutions. In order to give more insight about entropy-stabilized MO phases, the thermodynamic properties, including enthalpy of mixing (ΔH_{mix}) are calculated using eq. (2). During ΔH_{mix} calculations, stable phases of constituent 1-cationic oxides are considered. Although MO solid solutions are stable in the rocksalt phase, their constituent oxides are not always stable in that particular phase. NiO, CoO and MgO are stable in the rocksalt phase, while CuO and ZnO are

stable in the tenorite and wurtzite phases, respectively. According to eq. (2), if the oxide solid solutions possess negative ΔH_{mix} , oxide solid solution phases can be considered as enthalpy-wise more favorable compared to their constituent oxide phases. As observed from Fig. 2(a), MO-11 only exhibits low temperature stable phase. MO-12, MO-13 and MO-14 oxide solid solution phases exhibit positive ΔH_{mix} . The positive ΔH_{mix} values for MO-12, MO-13, and MO-14 indicate that the formation of a homogeneous rock-salt solid solution is not enthalpically preferred with respect to the selected binary oxide reference phases. This can be understood from the chemical and structural mismatch among the constituent cations. While NiO, CoO, and MgO naturally adopt rock-salt-type structures, CuO and ZnO prefer tenorite and wurtzite structures, respectively. Forcing these cations into a common rock-salt sublattice introduces an energetic penalty associated with local strain, bonding mismatch, and deviation from their preferred coordination environment. Thus, the increasing positive ΔH_{mix} from MO-12 to MO-14 reflects the increasing enthalpic cost of chemical complexity. In general, we can identify two different zones in the ΔH_{mix} plot. MO-11 belongs to a stable zone with $\Delta H_{mix} < 0$. MO-12, MO-13 and MO-14 belong to the unstable zone with $\Delta H_{mix} > 0$. Thus, MO-12, MO-13 and MO-14 oxide solid solution phases cannot be considered as enthalpy-stabilized phases. As the number of elements in the cationic site increases from MO-11 to MO-14, the corresponding decrease in the enthalpy-wise stability is observed. Negative (positive) values of ΔH_{mix} clearly indicate an exothermic (endothermic) reaction. Thus, the formation of medium entropy oxides MO-12, MO-13, and high entropy oxide: MO-14 involves the absorption of heat from external sources. Similarly, an endothermic formation energy indicates that reactants are thermodynamically more favorable. The progressive increase in positive ΔH_{mix} from MO-12 to MO-14 indicates that the incorporation of multiple

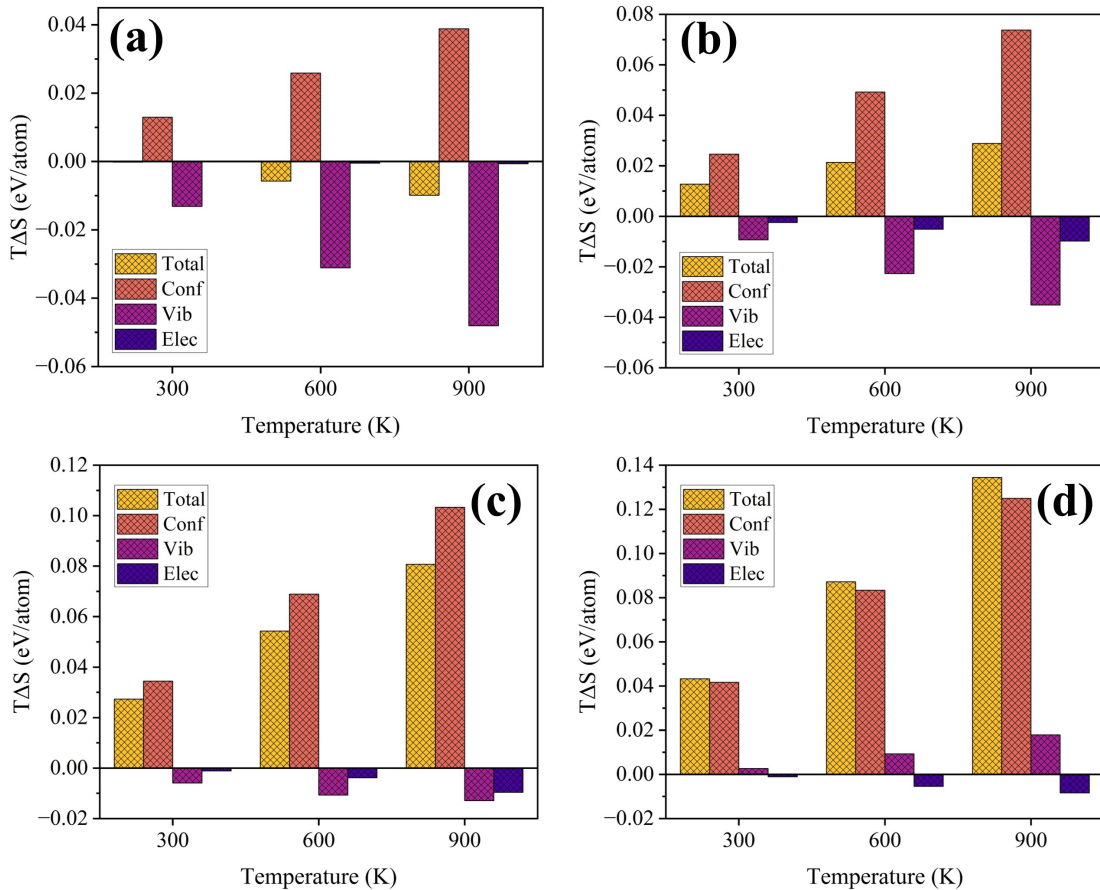


FIG. 3: Temperature dependent entropy contributions at three different temperatures 300 K, 600 K, 900 K for (a) MO-11, (b) MO-12, (c) MO-13 and (d) MO-14.

chemically and structurally dissimilar cations into a common rock-salt sublattice introduces increasing local strain and chemical mismatch. In particular, the coexistence of cations whose preferred binary oxides adopt different ground-state structures, such as tenorite CuO and wurtzite ZnO, imposes an energetic penalty when they are forced into the rock-salt lattice. Therefore, the high-temperature stability of these rock-salt oxide compositions cannot originate from enthalpic preference; rather, it must arise from entropy-driven lowering of the Gibbs free energy. Therefore, the stability of these multicomponent oxides cannot be inferred from ΔH_{mix} alone. The positive mixing enthalpy of MO-12, MO-13, and MO-14 establishes that entropy must play a decisive role if these compositions are to form stable single-phase rock-salt oxides at elevated temperature. This provides the basis for analyzing the configurational, vibrational, and electronic entropy contributions in the following section.

B. Entropy contribution

As our concern is to identify high-temperature stable phases, it is necessary to analyze the role of entropy towards exploring the change in Gibbs free energy (ΔG_{mix}) according to eq. (1). Change in Gibbs free energy not only involves ΔH_{mix} but also includes temperature multiplied by the entropy change (ΔS). In fact, the entropy change estimate includes contributions due to configuration degrees of freedom (DOF) (ΔS_{conf}), vibrational DOF (ΔS_{vib}) and electronic DOF (ΔS_{elec}). Configurational entropy is calculated based on fractional occupancy in the cationic site of MO as per eq. (3) [Fig. 2(b)]. A random oxide material can be classified as a high entropy oxide if it contains at least 5 or more elemental contributions in a single site ($S_{\text{conf}} \geq 1.5R$). Based on eq. (3), MO-14 is classified as high entropy oxide followed by MO-13 and MO-12 as medium entropy oxides [Fig. 2(b)]. This classification is based only on the magnitude of ideal configurational entropy. However, such a classification should not be directly equated with thermodynamic stability. A medium-entropy oxide may become entropy-stabilized if its positive ΔH_{mix} is suffi-

ciently compensated by the total entropy contribution at high temperature. Conversely, a high-entropy composition may still require a high stabilization temperature if the enthalpic penalty is large. Thus, ΔS_{conf} is a useful descriptor of compositional disorder, but it is not a complete predictor of phase stability.

The comparative contributions of electronic, vibrational and configurational entropy terms are shown in Fig. 3. In case of MO-11, contribution from electronic entropy term is negligible compared to vibrational and configurational entropy contributions throughout the temperature regime. Thus MO-11 exhibits a competition between vibrational and configurational entropy term. As around 300 K, these two terms contribute almost same, the total entropy term becomes negligible. However, as the temperature increases, corresponding vibrational entropy term contributes more, which results in the net nonzero $T\Delta S$. In all other oxides, from room temperature (300 K) onward, the total $T\Delta S$ term starts contributing. Starting from MO-12, the configurational entropy term starts dominating over vibrational and electronic entropy term. Configurational entropy term becomes significant in case of 4- and 5-cationic oxides like MO-13 and MO-14 respectively. Out of four oxide systems, MO-14 only possesses positive contribution from vibrational entropy term. The sign of ΔS_{vib} provides insight into how lattice dynamics change upon mixing. A positive ΔS_{vib} indicates that the multicomponent rock-salt phase has a larger vibrational entropy than the corresponding weighted binary oxide references, which may arise from phonon softening, mass disorder, and frustration in lattice geometry. This contribution further lowers ΔG_{mix} at elevated temperatures. In contrast, a negative ΔS_{vib} implies that the mixed phase is vibrationally less favorable than the reference oxides and therefore opposes entropy stabilization. Also, in case of 2- to 4-cationic oxides, the negative ΔS_{vib} acts as a penalty that the configurational entropy has to overcome. However, with the transition from 4- to 5-cationic oxide system, ΔS_{vib} acts synergistically with the configurational entropy working together to drastically lower the ΔG_{mix} and stabilize the single-phase rock-salt structure. Hence, vibrational entropy is not universally stabilizing; its effect depends on the relative phonon spectra of the solid solution and the reference phases. Due to that, the vibrational contribution along with significant configurational entropy term, total $T\Delta S$ contributes largely towards ΔG .

C. Gibbs free energy of solid solutions

Taking into consideration only the configurational entropy term, change in Gibbs free energy can be expressed as follows.

$$\Delta G_{\text{mix}}^{\text{conf}} = \Delta H_{\text{mix}} - T\Delta S_{\text{conf}} \quad (8)$$

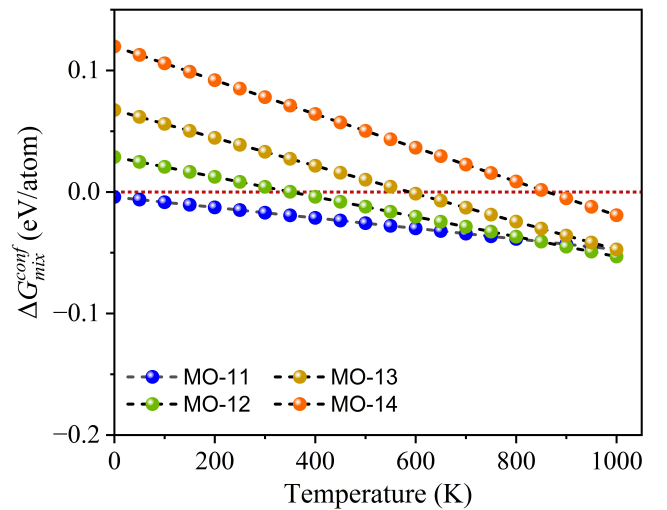


FIG. 4: Variation of Gibbs free energy change with temperature considering only configurational entropy change. Different MO systems are represented by different colors as indicated in the inset.

Fig. 4 depicts the variation $\Delta G_{\text{mix}}^{\text{conf}}$ as a function of temperature according to eq. 5. At 0 K, MO-12, MO-13, and MO-14 all have a positive enthalpy of mixing. However, when configurational entropy is taken into account, $\Delta G_{\text{mix}}^{\text{conf}}$ changes from positive to negative values at around 350 K (MO-12), 600 K (MO-13) and 850 K (MO-14), respectively. As the temperature increases further, MO-12 and MO-13 attain more negative $\Delta G_{\text{mix}}^{\text{conf}}$ with a value of > 20 meV/atom at 1000 K temperature. The inclusion of the configurational entropy term, $T\Delta S_{\text{conf}}$ does not guarantee the high-temperature stability of these oxides. The $\Delta G_{\text{mix}}^{\text{conf}}$ analysis demonstrates the stabilizing tendency of configurational entropy, but it also highlights the limitation of using ΔS_{conf} alone. Since the actual free energy contains vibrational and electronic entropy contributions, a stability criterion based only on ΔS_{conf} may either overestimate or underestimate the stabilization temperature. Therefore, the total Gibbs free energy including ΔS_{conf} , ΔS_{vib} , and ΔS_{elec} provides a more reliable thermodynamic description. To give more insight about high-temperature stability of these oxides, it is necessary to include other possible contributions towards the entropy change. In fact, taking into consideration electronic and vibrational contributions, the change in Gibbs free energy of mixing can be written as follows.

$$\Delta G_{\text{mix}} = \Delta H_{\text{mix}} - T\Delta S_{\text{conf}} - T\Delta S_{\text{vib}} - T\Delta S_{\text{elec}} \quad (9)$$

Here $T\Delta S_{\text{vib}}$ and $T\Delta S_{\text{elec}}$ represent entropy change due to lattice vibrations and electronic contributions respectively. Fig. 5(a) depicts the variations of ΔG_{mix} with temperature including all possible entropic contributions for MO-11.

A very small difference between ΔG_{mix} and $\Delta G_{\text{mix}}^{\text{elec}}$ is observed around high-temperature, which basically

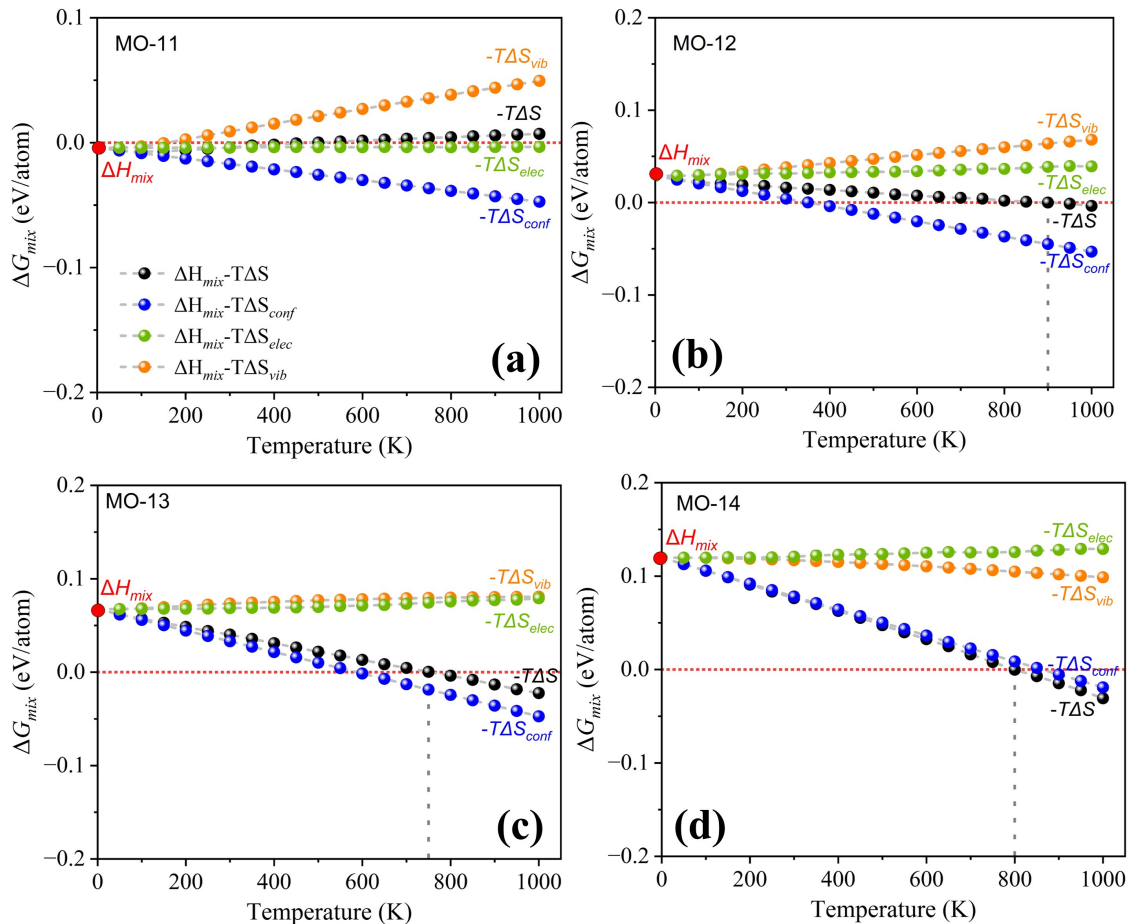


FIG. 5: Variations of Gibbs free energy change due to mixing as a function of temperature for (a) MO-11, (b) MO-12, (c) MO-13 and (d) MO-14 systems. Corresponding individual contributions are represented by different colors as indicated in the inset.

arises due to the competition between vibrational and configurational entropy contributions. Around room temperature, both the contributions are similar. However, with increasing temperature, the vibrational term contributes more in the negative regime, in such a way that ΔG_{mix} becomes positive even at a high-temperature of 1000 K. Thus with all possible entropy consideration, MO-11 becomes an unstable phase at high-temperature regime. A different scenario is observed in case of other MO systems. MO-12 possesses a positive ΔH_{mix} at 0 K temperature. However with increasing temperature as the entropy terms are included, ΔG_{mix} goes through a transition from positive to negative values at a temperature of 850 K. Around both low and high-temperature regime, the configurational contribution becomes twice that of the vibrational contribution [Fig. 5(b)]. Around 1000 K temperature, considering all entropy contributions, MO-12 possesses a negative ΔG_{mix} of 3.58 meV/atom. Thus, contrary to enthalpy-stabilized MO-11, MO-12 oxide phase can be considered entropy-stabilized and thermodynamically stable. MO-13 exhibits negative

values of both $T\Delta S_{vib}$ and $T\Delta S_{elec}$ throughout the temperature regime. Around high-temperature, vibrational entropy contribution is quite comparable with the electronic entropy contribution. Thus, considering the vibrational and electronic entropy contributions, ΔG_{mix} shows more positive values compared to ΔH_{mix} at higher temperature. However, significant contribution from configurational entropy makes transition of the ΔG_{mix} from positive to negative at $T \geq 750$ K [Fig. 5(c)]. Thus 3- and 4-cationic oxide systems such as MO-12 and MO-13 can possess significant configurational entropy which can assure their entropy-stabilized high-temperature stability. On the other hand, because of high positive ΔH_{mix} , MO-14 is considered as enthalpy-wise unstable phase as 0 K. In addition, being a 5-cationic oxide system, MO-14 exhibits the highest configurational entropy (1.61 R) contribution among all oxide systems considered in this study. Because of that main contribution in $T\Delta S$ comes from configurational entropy. As the temperature increases, vibrational term $T\Delta S_{vib}$ also contributes significantly in $T\Delta S$ [Fig. 5(d)]. In the high-temperature regime, the large

positive contributions of $T\Delta S_{conf}$ and $T\Delta S_{vib}$ projects $T\Delta S$ to a significant quantity. This $T\Delta S$ is sufficient enough to offer a transition of ΔG_{mix} from positive to negative values around 800 K. Further around 1000 K temperature, ΔG_{mix} reaches more negative value of -31 meV/atom. As MO-11 exhibits positive ΔG_{mix} , it cannot be considered as stable around high-temperature. On the other hand, although having high positive ΔH_{mix} , MO-14 exhibit significant negative ΔG_{mix} around high-temperature because of high configurational entropy. Thus MO-14 offers thermodynamically stable high entropy phase. Even MO-12 and MO-13 having medium configurational entropy, can also offer high-temperature entropy-stabilized and thermodynamically stable phases. Overall, these results demonstrate that entropy stabilization in rock-salt oxides should not be reduced to a fixed configurational entropy threshold. The conventional $\Delta S_{conf} \geq 1.5R$ criterion is useful for classifying high-entropy compositions, but it does not by itself establish entropy-stabilized phase formation. The formation of a single-phase rock-salt oxide is governed by the balance between the enthalpic penalty associated with incorporating chemically distinct cations into a common lattice and the total entropy gain available at elevated temperature. In this framework, MO-12 and MO-13 are particularly important because they show that medium-entropy compositions can become stable when their moderate positive ΔH_{mix} is compensated by configurational and non-configurational entropy terms. [5, 7, 28] MO-14, although having the largest ΔS_{conf} , also possesses the largest enthalpic penalty, showing that high entropy and high stability are not necessarily equivalent. This conclusion is consistent with recent experimental reports on quaternary medium-entropy rock-salt oxides.[28] For example, single-phase $(Mg_{0.25}Co_{0.25}Ni_{0.25}Zn_{0.25})O$ has been synthesized in the 1000–1200 °C temperature range and shown to possess good thermal stability. Such studies support the idea that the five-cation high-entropy condition is not a strict requirement for stabilizing rock-salt oxide solid solutions.[7, 13, 29] The present calculations provide a thermodynamic basis for this observation by showing that medium-entropy compositions can also reach negative ΔG_{mix} at elevated temperature and is in line with the recent observation made experimentally[30]. It should be noted that the present analysis evaluates phase stability with respect to selected binary oxide reference phases. In real multicomponent oxides, additional competing polymorphs, partially segregated phases, ternary phases, local short-range ordering, and oxygen non-stoichiometry may influence the equilibrium phase field. Furthermore, the experimentally observed room-temperature phase assemblage may depend strongly on synthesis temperature, annealing time, cooling rate, and cation diffusion kinetics. Therefore, the calculated $\Delta G_{mix} < 0$ condition should be interpreted as a thermodynamic indicator of high-temperature single-phase stability rather than an exact prediction

of synthesis temperature or retained room-temperature phase stability.[6, 7, 13, 29]

III. CONCLUSION

In conclusion, using a first-principles-based thermodynamic framework, we systematically investigated the temperature-dependent phase stability of rock-salt oxide solid solutions containing two to five principal cation components, denoted as MO-11 to MO-14. The mixing enthalpy indicate -ve values for MO-11 at 0K, whereas MO-12, MO-13, and MO-14 exhibit positive ΔH_{mix} , indicating that their homogeneous rock-salt solid-solution formation is not enthalpically favored with respect to the selected binary oxide reference phases. The Gibbs free-energy analysis reveals that the stability picture based on 0K enthalpy changes significantly at finite temperature. MO-11, despite being enthalpy-stabilized at low temperature, shows positive ΔG_{mix} at elevated temperature and therefore does not remain thermodynamically stable in the high-temperature regime. In contrast, MO-12, MO-13, and MO-14 become thermodynamically stable at high temperature due to entropy-driven lowering of ΔG_{mix} . Among the entropy terms, vibrational entropy dominates in MO-11, whereas configurational entropy provides the major stabilizing contribution in MO-12, MO-13, and MO-14, with additional contributions from vibrational and electronic entropy. These results demonstrate that configurational entropy alone is not a universal criterion for phase stabilization. Although MO-14 satisfies the conventional high-entropy condition with $\Delta S_{conf} \approx 1.61R$, its large positive ΔH_{mix} reflects a substantial enthalpic penalty. Conversely, MO-12 and MO-13, despite belonging to the medium-entropy regime, become stable because their moderate positive ΔH_{mix} is overcome by the total entropy contribution at elevated temperature. Thus, the design of compositionally complex rock-salt oxides should be guided by the full ΔG_{mix} balance rather than by the conventional five-cation or $\Delta S_{conf} \geq 1.5R$ criterion alone. Finally, the present analysis considers thermodynamic stability only with respect to decomposition into selected stable binary oxide phases. Kinetic effects, oxygen non-stoichiometry (which can introduce additional configurational entropy on the anion sublattice), cation short-range ordering (SRO), magnetic entropy, defect formation, and possible competing ternary or intermediate phases are not explicitly included in this model. Therefore, the predicted stabilization temperatures serve as idealized thermodynamic indicators rather than exact synthetic boundaries.

IV. DECLARATION OF COMPETING INTEREST

The authors declare that they have no known competing financial interests or personal relationships that could have appeared to influence the work reported in the paper.

V. AUTHOR CONTRIBUTION STATEMENT

SG Simulation, Formal analysis, Writing original draft. **AK**: Conceptualization, Formal Analysis, Writing-review and edit-

ing. **SKP**: Conceptualization, Discussions, Supervision, Finalizing manuscript.

VI. ACKNOWLEDGMENT

SG sincerely acknowledges ANRF, Govt. of India (File number: PDF/2025/001037) for providing NPDF fellowship. SKP acknowledges ANRF JC Bose Fellowship and ANRF, Govt. of India for the Financial support. SG and SKP would like to thank the National Supercomputing Mission, PARAM Yukti facilities for providing computational resources.

-
- [1] C. M. Rost, E. Sachet, T. Borman, A. Moballeghe, E. C. Dickey, D. Hou, J. L. Jones, S. Curtarolo, J.-P. Maria, Entropy-stabilized oxides, *Nature communications* 6 (1) (2015) 8485.
- [2] A. Kumar, D. Bérardan, F. Brisset, D. Dragoe, N. Dragoe, Novel entropy-stabilized fluorite oxides with multifunctional properties, *Journal of Materials Chemistry A* 11 (26) (2023) 14320–14332.
- [3] F. Vayer, C. Decorse, D. Berardan, N. Dragoe, New entropy-stabilized oxide with pyrochlore structure: Dy₂(Ti_{0.2}Zr_{0.2}Hf_{0.2}Ge_{0.2}Sn_{0.2})₂O₇, *Journal of Alloys and Compounds* 883 (2021) 160773.
- [4] L. Spiridigliozzi, M. Biesuz, V. Sglavo, G. Dell’Agli, Design, synthesis and formation mechanism of a novel entropy-stabilized perovskite oxide derived from barium cerate/zirconate, *Journal of the European Ceramic Society* 44 (4) (2024) 2223–2232.
- [5] M. Fracchia, M. Coduri, M. Manzoli, P. Ghigna, U. A. Tamburini, Is configurational entropy the main stabilizing term in rock-salt Mg_{0.2}Co_{0.2}Ni_{0.2}Cu_{0.2}Zn_{0.2}O high entropy oxide?, *Nature Communications* 13 (1) (2022) 2977.
- [6] R. J. Spurling, E. A. Lass, X. Wang, K. Page, Entropy-driven phase transitions in complex ceramic oxides, *Physical Review Materials* 6 (9) (2022) 090301.
- [7] S. S. Aamlid, M. Oudah, J. Rottler, A. M. Hallas, Understanding the role of entropy in high entropy oxides, *Journal of the American Chemical Society* 145 (11) (2023) 5991–6006.
- [8] A. Kumar, D. Bérardan, D. Dragoe, E. Riviere, T. Takayama, H. Takagi, N. Dragoe, Magnetic and electrical properties of high-entropy rare-earth manganites, *Materials Today Physics* 32 (2023) 101026.
- [9] A. Kumar, A. Moll, M. N. Mouhamadsiradjoudine, F. Brisset, D. Berardan, N. Dragoe, Thermoelectric properties of high-entropy wolframite oxide:(cocunifezn) 1-xgaxwo4, *physica status solidi (RRL)–Rapid Research Letters* 18 (3) (2024) 2300372.
- [10] M. Brahlek, M. Gazda, V. Keppens, A. R. Mazza, S. J. McCormack, A. Mielewczyk-Gryń, B. Musico, K. Page, C. M. Rost, S. B. Sinnott, et al., What is in a name: Defining “high entropy” oxides, *APL Materials* 10 (11) (2022).
- [11] J. T. Sivak, S. S. Almishal, M. K. Caucci, Y. Tan, D. Srikanth, J. Petruska, M. Furst, L.-Q. Chen, C. M. Rost, J.-P. Maria, et al., Discovering high-entropy oxides with a machine-learning interatomic potential, *Physical review letters* 134 (21) (2025) 216101.
- [12] S. Divilov, H. Eckert, D. Hicks, C. Oses, C. Toher, R. Friedrich, M. Esters, M. J. Mehl, A. C. Zettl, Y. Lederer, et al., Disordered enthalpy–entropy descriptor for high-entropy ceramics discovery, *Nature* 625 (7993) (2024) 66–73.
- [13] A. F. Manchón-Gordón, P. Panadero-Medianero, J. S. Blázquez, Descriptors for predicting single-and multi-phase formation in high-entropy oxides: A unified framework approach, *Materials* 18 (16) (2025) 3862.
- [14] G. Kresse, J. Hafner, Ab initio molecular dynamics for liquid metals, *Phys. Rev. B* 47 (1) (1993) 558.
- [15] G. Kresse, J. Hafner, Ab initio molecular-dynamics simulation of the liquid-metal–amorphous-semiconductor transition in germanium, *Physical Review B* 49 (20) (1994) 14251.
- [16] G. Kresse, J. Furthmüller, Efficiency of ab-initio total energy calculations for metals and semiconductors using a plane-wave basis set, *Computational Materials Science* 6 (1) (1996) 15–50.
- [17] P. E. Blöchl, Projector augmented-wave method, *Phys. Rev. B* 50 (1994) 17953–17979.
- [18] J. P. Perdew, K. Burke, M. Ernzerhof, Generalized gradient approximation made simple, *Phys. Rev. Lett.* 77 (18) (1996) 3865.
- [19] H. J. Monkhorst, J. D. Pack, Special points for brillouin-zone integrations, *Phys. Rev. B* 13 (1976) 5188–5192.
- [20] E. Konysheva, E. Suard, J. T. Irvine, Effect of oxygen non stoichiometry and oxidation state of transition elements on high-temperature phase transition in a-site deficient La_{0.95}Ni_{0.6}Fe_{0.4}δ perovskite, *Chemistry of Materials* 21 (21) (2009) 5307–5318.
- [21] A. Zunger, S.-H. Wei, L. G. Ferreira, J. E. Bernard, Special quasirandom structures, *Physical review letters* 65 (3) (1990) 353.
- [22] A. Van De Walle, M. Asta, G. Ceder, The alloy theoretic automated toolkit: A user guide, *Calphad* 26 (4) (2002) 539–553.
- [23] A. Van De Walle, Multicomponent multisublattice alloys, nonconfigurational entropy and other additions to the alloy theoretic automated toolkit, *Calphad* 33 (2) (2009) 266–278.
- [24] A. van de Walle, P. Tiwary, M. de Jong, D. L. Olmsted, M. Asta, A. Dick, D. Shin, Y. Wang, L.-Q. Chen, Z.-K. Liu, Efficient stochastic generation of special quasirandom structures, *Calphad* 42 (2013) 13–18.
- [25] A. Manzoor, S. Pandey, D. Chakraborty, S. R. Phillpot,

- D. S. Aidhy, Entropy contributions to phase stability in binary random solid solutions, *npj Computational Materials* 4 (1) (2018) 47.
- [26] A. Togo, First-principles phonon calculations with phonopy and phono3py, *Journal of the Physical Society of Japan* 92 (1) (2023) 012001.
- [27] A. Togo, I. Tanaka, First principles phonon calculations in materials science, *Scripta materialia* 108 (2015) 1–5.
- [28] Z. He, W. Xuan, T. Hu, G. Zhang, J. Chen, Q. Zhang, G. Shao, H. Song, Z. Ren, Development of a novel (mg_{0.25}co_{0.25}ni_{0.25}zn_{0.25}) o medium entropy oxide for dielectric applications, *Ceramics International* 50 (17) (2024) 31598–31608.
- [29] K. C. Pitike, S. Kc, M. Eisenbach, C. A. Bridges, V. R. Cooper, Predicting the phase stability of multicomponent high-entropy compounds, *Chemistry of Materials* 32 (17) (2020) 7507–7515.
- [30] A. Kumar, A. Moll, J. Kumar, D. Dragoë, D. Bérardan, N. Dragoë, Configurational entropy-driven phase stability and thermal transport in rock-salt high-entropy oxides, *arXiv preprint arXiv:2510.09342* (2025).